Available online at www.sciencedirect.com
SCIENCE DIRECT®
Biosensors and Bioelectronics 20 (2004) 606–619
BIOSENSORS & BIOELECTRONICS
www.elsevier.com/locate/bios

Electronic manipulation of DNA, proteins, and nanoparticles for potential circuit assembly

Lifeng Zheng [a], James P. Brody [b], Peter J. Burke [a,b,*]

[a] *Electrical Engineering and Computer Science, University of California, Irvine, CA 92697-2625, USA*
[b] *Biomedical Engineering, University of California, Irvine, CA 92697-2625, USA*

Received 29 October 2003; received in revised form 8 March 2004; accepted 8 March 2004
Available online 24 May 2004

Abstract

Using gold electrodes lithographically fabricated onto microscope cover slips, DNA and proteins are interrogated both optically (through fluorescence) and electronically (through conductance measurements). Dielectrophoresis is used to position the DNA and proteins at well-defined positions on a chip. Quadrupole electrode geometries are investigated with gaps ranging from 3 to 100 μm; field strengths are typically 10^6 V/m. Twenty nanometer latex beads are also manipulated. The electrical resistance of the electronically manipulated DNA and proteins is measured to be larger than 40 MΩ under the experimental conditions used. The technique of simultaneously measuring resistance while using dielectrophoresis to trap nanoscale objects should find broad applicability.

Keywords: Dielectrophoresis; DNA; Proteins; Nanoparticles

1. Introduction

1.1. Motivation

The development of lithographic fabrication techniques has lead to astounding advances in integrated circuits, but at the same time the limits of lithography prevent nanometer scale electronic devices from being economically manufactured. This has led to proposals for alternative nanomanufacturing technologies based on "bottom-up" chemical self-assembly techniques.

Two key challenges in the manufacturing of sub-lithographic size electronic devices (i.e. molecular electronics (Heath and Ratner, 2003)) are (1) chemical (i.e. bottom-up) control of the electronic properties of the circuit elements, and (2) electrical connection to the macroscopic world. One approach to the challenge of chemical control is *de-novo* design of unique chemistry for electronics applications (Tour, 2000; Luo et al., 2002). An alternative approach is to build on 4 billion years of evolution and use or mimic existing biochemistry, using DNA as a template for chemically programmed assembly of molecular scale devices. Recently several groups have made important progress in using DNA as a template for the construction of higher order structures (Braun et al., 1998; Winfree et al., 1998; Mirkin et al., 1996; Alivisatos et al., 1996). Because of the attractiveness of the second approach we have decided to concentrate on the electronic manipulation and interrogation of DNA and proteins in this work.

The second challenge of making an electrical connection to the macroscopic world to date has mostly been achieved passively. Much work to date on single molecule devices involves passive diffusion of molecules to small, albeit lithographically fabricated electrodes followed by passive covalent bonding to the electrode (Chen and Reed, 2002). It would be a distinct advantage if this assembly process could be actively, electronically controlled.

1.2. Dielectrophoresis

Dielectrophoresis (hereafter DEP) is an electronic analog of optical tweezers using audio frequency, rf, and microwave electric fields generated from microfabricated electrodes on a chip. An ac electric field induces a dipole moment which,

* Corresponding author. Tel.: +1-949-824-9326; fax: +1-949-824-3782.
E-mail address: pburke@uci.edu (P.J. Burke).

0956-5663/$ – see front matter © 2004 Elsevier B.V. All rights reserved.
doi:10.1016/j.bios.2004.03.029

in the presence of a field gradient, experiences a force towards either the high-field intensity region (positive DEP) or the low-field intensity region (negative DEP). Several recent reviews more thoroughly describe the many applications of DEP at the micron, sub-micron, and nanometer scale (Pethig, 1996; Pethig and Markx, 1997; Zimmermann and Neil, 1996; Ramos et al., 1998; Green et al., 2000; Hughes, 2000; Burke, 2004). As with optical tweezers, for DEP to be of use it must dominate the thermal Brownian motion.

It can be shown that the force acting on a spherical particle (the DEP force) is given by (Pohl, 1978; Jones, 1995)

$$\vec{F}_{\mathrm{DEP}} = 2\pi v \varepsilon_{\mathrm{m}} K(\omega) \vec{\nabla}(\vec{E}^2_{\mathrm{RMS}}), \tag{1}$$

where v is the volume of the particle, E_{RMS} the RMS value of the electric field (assuming a sinusoidal time dependence), and $K(\omega)$ is a (frequency dependent) factor which varies between -0.5 and $+1.0$, depending on the difference between the medium and particle dielectric constant. It is defined as

$$K(\omega) \equiv Re\left(\frac{\varepsilon^*_{\mathrm{p}} - \varepsilon^*_{\mathrm{m}}}{\varepsilon^*_{\mathrm{p}} + 2\varepsilon^*_{\mathrm{m}}}\right), \tag{2}$$

where ε^* is the (complex) dielectric constant of the particle or medium. It can be related to the conductivity σ and angular frequency ω through the standard formula

$$\varepsilon^* \equiv \varepsilon - \mathrm{i}\frac{\sigma}{\omega}. \tag{3}$$

$K(\omega)$ is known as the Clausius–Mossotti factor. If $K(\omega)$ is positive, then the particle is attracted to regions of high electric field intensity. (This is called positive DEP.) If $K(\omega)$ is negative, then the particle is repelled from regions of high electric field intensity. (This is called negative DEP.) Since $K(\omega)$ is frequency dependent, both positive and negative DEP can be observed in the same system by varying the frequency.

Although the above analysis assumes a harmonic field, the physical effect is present for dc electric fields as well: a dc electric field can induce a dipole moment, which then experiences a force in the presence of a field gradient. We term this effect dc DEP.

In principle, quantitative measurements of the force predicted by Eq. (1) are possible. However, a more direct measurement often used is the frequency at which the force changes from positive to negative DEP. In experiments, the frequency is varied until the particle motion is no longer towards low-field intensity, and instead is towards high-field intensity regions; this is straightforward to observe. For a spherical particle, it can be shown that this frequency, called the "crossover frequency", is given by (Morgan and Green, 2003):

$$f_{x\text{-over}} = \frac{1}{2\pi}\sqrt{-\frac{(\sigma_{\mathrm{p}} - \sigma_{\mathrm{m}})(\sigma_{\mathrm{p}} + 2\sigma_{\mathrm{m}})}{(\varepsilon_{\mathrm{p}} - \varepsilon_{\mathrm{m}})(\varepsilon_{\mathrm{p}} + 2\varepsilon_{\mathrm{m}})}}. \tag{4}$$

In Eqs. (1)–(3), the values of ε^* and σ are assumed to be the bulk values. For nanoparticles and biological nanostructures such as DNA, a significant fraction of the atoms of the "particle" reside on the surface; in addition, the particles can be charged. For example, at neutral pH, DNA is negatively charged. Protons and any other positively charged counter-ions are attracted and form a counter-ion cloud. Clearly, the corresponding electrical double layer (consisting of the positively charged counter-ion cloud and the negatively charged particle) can have a significant effect on DEP.

The effects of the double layer on the dielectric properties of colloidal solutions of dielectric particles was considered theoretically on very general grounds in several key papers in the 1960s and refined in the 1980s (Okonski, 1960; Schwarz, 1962; Lyklema et al., 1983, 1986; Lyklema, 2000). While these authors concentrated on dielectric properties, they did not discuss DEP. In the late 1990s, Green and Morgan performed extensive experimental investigations on latex beads down to 93 nm in diameter, varying the frequency, surface chemistry, and electrolyte conductivity (Green and Morgan, 1997a,b, 1998, 1999; Hughes and Morgan, 1999; Hughes et al., 1999a,b; Hughes, 2002; Hughes and Green, 2002). They based the interpretation of the experiments on the earlier theories of the charge double layer. The conclusions of their results can be summarized as follows: the effects of the charge double layer are to incorporate a surface conductance due to the motion of either bound counter-ions (the Stern layer) or diffuse counter-ions, with numerical value given by K_{s}. Eqs. (1)–(4) are still valid, provided that the total particle conductivity in Eq. (3) be replaced with

$$\sigma_{\mathrm{p}} = \sigma_{\mathrm{b}} - \frac{2K_{\mathrm{s}}}{a}. \tag{5}$$

Here a is the particle radius and σ_{b} the bulk conductance. Generally speaking, Eq. (5) should only be used if the frequency is less than the inverse of the diffusion time of ions across a distance of order a. If this is not the case, then Eq. (5) should be modified.

For this force to be effective it must overcome the Brownian motion, which can be treated as a random force whose maximum value is given roughly by

$$F_{\mathrm{thermal}} = \frac{k_{\mathrm{B}}T}{\sqrt[3]{v}}, \tag{6}$$

where k_{B} is the Boltzmann constant, T the temperature, and v the particle volume. This sets a rather strict requirement on the minimum particle size that can be manipulated, and very large electric field gradients are needed to manipulate nanosized particles. Microfabricated electrodes can be used to generate the required field gradients, although the lower limit on the particle size that can be manipulated is still under experimental investigation (Zheng et al., 2003).

1.3. Dielectrophoretic impedance spectroscopy

While deterministic motion of individual molecules due to DEP is difficult to achieve due to Brownian motion, it

is still true that the non-uniform ac and dc electric fields establish some force, which, even though less than the thermal Brownian motion, will still cause a tendency for molecules to move in a certain direction, depending on the geometry of the electrodes. The quantitative study of these effects has been termed "molecular DEP" (Pohl, 1978). The establishment of impedance spectroscopy essentially consists of measuring the ac impedance between two electrodes at a probe frequency while DEP is used to manipulate objects at a separate frequency. This technique was originally pioneered over 50 years ago.

The geometry originally studied consists of two concentric cylinders with the molecules dissolved in a solution in between the cylinders. If the density of the molecules as a function of the radial distance changes, this changes the dielectric constant as a function of the radius, and hence the capacitance from the inner to the outer cylindrical electrode. This can be termed a form of dielectrophoretic impedance spectroscopy.

In 1954, Debye et al. used dc DEP of polystyrene (molecular weight 600,000) in cyclohexane (Debye et al., 1954a,b). They used a dc non-uniform electric field in a cylindrical geometry and monitored the capacitance change by measuring the shift in the resonant frequency of an LC circuit; similar studies were carried out by Prock in 1960 (Prock and Mcconkey, 1960).

In 1955, Losche (Losche and Hultschig, 1955) used ac DEP to study nitrobenzene in carbon tetrachloride, and poly(vinyl acetate) in nitrobenzene; however both have permanent (instead of induced) dipoles. In 1973 Eisenstadt (Eisenstadt and Scheinberg, 1972, 1973) studied DEP and measured the diffusion constant of the biopolymers poly-γ-benzyl-L-glutamate (PBLG, MW 120,000) and poly-*n*-butyl isocyanate dissolved in ethylene dichloride (Edc); both have permanent dipoles. By measuring the time-dependence of the concentration change of the PBLG concentration due to the dielectrophoretic force, Eisenstadt was able to determine its diffusion constant.

Recently, Milner et al. have extended dielectrophoretic impedance spectroscopy to larger particles which can be deterministically manipulated with DEP. They used DEP to position bacteria (Milner et al., 1998; Allsopp et al., 1999) or 20 nm latex beads (Brown et al., 1998) with high frequency (kHz to MHz) electric fields, and simultaneously measured the low frequency (∼100 Hz) impedance between two electrodes.

Thus, there is an extensive history and established technology to use DEP to manipulate a variety of objects (molecules, nanoparticles, cells) at one frequency, and to use a different probe frequency to measure the impedance change when the objects are moved. However, all of the examples cited above cause a change in the *capacitance* between the electrodes. Hence, the probe frequency could not be too low. Our work in this manuscript addresses a related but somewhat different goal: we are interested in using DEP to fabricate circuits that function at dc. As we discuss next, there are a many examples from the literature demonstrating that this can be done.

1.4. DEP for nanocircuit fabrication

To date there have been several examples of the application of DEP to circuit fabrication at the nanometer scale. Suehiro (Suehiro et al., 1999) measured the resistance and capacitance between two electrodes at 100 kHz before and after bacteria cells were trapped using DEP; he modeled each cell as a resistor in parallel with a capacitor and found good agreement with experiment: the cells formed "pearl chains" and bridged the gap between the two electrodes. Bezryadin used (dc) DEP to trap a 20 nm Pd nanoparticle between a two electrodes, allowing current to flow at dc (Bezryadin et al., 1997; Bezryadin and Dekker, 1997). Bezryadin later used DEP to trap carbon nanoparticles between electrodes in pearl-chain formation, and measured non-linear dc *I–V* curves due to Coulomb blockade (Bezryadin et al., 1999). Amlani used DEP to trap a Au nanoparticle coated with a self-assembled monolayer (SAM), and he observed negative differential resistance at dc from electrode to electrode due to the SAM (Amlani et al., 2002). Porath used dc DEP to trap short strands of DNA and measured the conductance of DNA so trapped (Porath et al., 2000). Velev used DEP to assemble microwires from nanoparticles and measured dc current through these (Bhatt and Velev, 2004; Hermanson et al., 2001). We recently use carbon nanotubes as electrodes to assemble gold nanowires from nanoparticles (Zheng et al., 2004b). Several groups have used both ac and dc DEP to trap single walled and multiwalled carbon nanotubes between electrodes which then carry dc current (Bezryadin and Dekker, 1997; Yamamoto et al., 1996, 1998; Wakaya et al., 2002; Chen et al., 2001; Bubke et al., 1997; Nagahara et al., 2002; Diehl et al., 2001). Smith used DEP to assemble gold nanowires across electrodes, which then carried dc current (Smith et al., 2000). Duan assembled functional crossbar networks of semiconducting nanowires using dc DEP (Duan et al., 2001). Lee and Bashir measured Si resistors at dc after using ac DEP to position them between electrodes (Lee and Bashir, 2003). To date no authors have used ac DEP to manipulate DNA then measure conductance between two electrodes, and no authors have measured any protein conductance after DEP manipulation, as we do in this manuscript. Our work in this manuscript thus represents the first step towards extending DEP for circuit fabrication into the molecular domain.

1.5. DNA manipulation: Washizu

Starting in 1990, Washizu and Kurosawa began studies on manipulating and stretching DNA in high intensity ac electric fields between 40 kHz and 2 MHz generated by microfabricated electrodes (Washizu and Kurosawa, 1990). They found that a high-frequency electric field would stretch DNA

into a line, whereas its natural configuration is coiled. In 1995, Washizu et al. described several possible applications of this technology (Washizu et al., 1995), such as size-sorting long DNA (length > 10 kbp) which is difficult for conventional gel electrophoresis, laser cutting of DNA with spatial resolution determined optically, and measurements of the rate of exonuclease DNA digestion. Further work by Washizu et al. used DEP and showed, for example, that RNA polymerase actually slides along DNA molecules during genetic expression (Kabata et al., 1993, 2000; Shimamoto, 1999), that DEP works at the single DNA molecule level, not on aggregates (Ueda et al., 1999a), restriction enzyme cutting of DNA oriented using DEP (Yamamoto et al., 2000), and the polarization of the fluorescent emission from dielectrophoretically stretched DNA (Suzuki et al., 1998). In spite of all this outstanding experimental work, very little explanation was given of the electrical double layer in the DNA.

1.6. DNA manipulation: other groups

Since Washizu's pioneering experiments in the early 1990s, several other groups have convincingly demonstrated the dielectrophoretic manipulation of DNA. Asbury and coworkers were able to manipulate DNA with a floating Au electrode geometry (Asbury and van den Engh, 1998; Asbury et al., 2002) using frequencies between 5 Hz and 2 kHz. In contrast to Washizu's experiments which clearly showed DNA to be stretched by DEP using higher frequencies, Asbury found for the lower frequency DEP can position DNA but does not stretch it.

Ueda et al. found that DNA could be stretched but not positioned when a polymer solution (polyacrylamide) was used (Ueda et al., 1997, 1999b); 10 Hz was the frequency used. They also found the required electric field strength to be 100 times smaller than that of Washizu and Asbury.

In another recent work with floating electrodes, Chou et al. (Chou et al., 2002) used insulating posts fabricated with micromachining techniques, and electrodes external to the device. The slightly conductive solution served to enhance the electric field near the gaps between the posts, and DNA was found to be trapped there for voltages on the electrodes of roughly 1000 V and frequencies between 50 Hz and 1 kHz. The corresponding electric field strength was 10^5 V/m. In this work, the DNA was apparently not stretched at all, presumably because of the constricted geometry used. In contrast to the work of Asbury, Chou found that the trapping force increased with increasing frequency, and also calculated that the trapping force was roughly one femtonewton.

In recent work (Tsukahara et al., 2001) Tsukahara et al. studied DEP of single DNA molecules using frequencies between 1 kHz and 1 MHz and field strengths around 10^4 V/m, using quadrupole electrode geometries. They found that the DNA underwent positive DEP (i.e. it was attracted to the high field regions near the edges of the electrodes) for frequencies between 1 kHz and 500 kHz, and negative DEP between 500 kHz and 1 MHz, in contrast with the findings of previous work. This is to date the only reported observation of negative DEP of DNA. Additionally, Tsukahara did not observe any stretching of the DNA with the application of an ac electric field.

Namasivayam et al. recently used 1 MHz ac fields and thiol modified DNA to trap single DNA molecules to gold electrodes; they studied the stretching as a function of polyacrylamide concentration (Namasivayam et al., 2002). Holzel and coworkers also recently used DEP at 2 MHz and selective electrode functionalization to vectorially orient DNA molecules which bridged a gap between electrodes (Holzel et al., 2003; Holzel and Bier, 2003). Germishuizen et al. oriented (stretched) surface immobilized DNA using 80 kHz to 1.1 MHz DEP (Germishuizen et al., 2003a,b) Recently, Dewarrat et al. optimized the geometry of the lithographic structures to favor a precise positioning of DNA using 100 kHz to 1 MHz (Dewarrat et al., 2002).

The detailed mechanisms for the frequency dependence, electric field dependence, concentration dependence, pH and ionic dependence of the dielectrophoretic manipulation of DNA are still not explained in a systematic, quantitative way, and many of these dependences have yet to be quantitatively measured. In addition, none of these authors have measured the electrical properties of the DNA after manipulation.

1.7. DNA and proteins: electrical properties

Thus, while most of this research work focused on manipulating DNA and proteins, investigation of their electrical properties is still in its infancy. In 2000, Porath et al. used positive dc DEP to putatively trap 10 nm long poly(G)–poly(C) double strands of DNA between Pt electrodes with 8 nm spacing (Porath et al., 2000). Through a series of control experiments, Porath concluded that the trapped object was indeed DNA, and that its electrical properties were semiconducting. Many other researchers up to and since then have considered the electronic properties of DNA as a molecular wire. Since then, experiments performed by different research groups have indicated that DNA has insulating, semiconducting, metallic and even superconducting properties (de Pablo et al., 2000; Storm et al., 2001; Porath et al., 2000; Cai et al., 2000; Okahata et al., 1998; Fink and Schonenberger, 1999; Kasumov et al., 2001).

These differing results of the electrical properties of DNA indicate that effective methods should be set up for the measurements. As for the electrical properties of proteins, these biological nanostructures have yet (until now) to be interrogated electrically. Our work in this paper represents the first step in this direction. Since various proteins have many differing chemical and mechanical properties, it can be argued that their electrical properties will be even more diverse (and hence interesting) than those of DNA.

1.8. This research work

In this work, a technique is presented that may be useful for the electronic control of manufacturing devices at the molecular scale by controlling the position of DNA and proteins on a chip to fabricate simple electrical circuits (a conductor bridging a gap). We apply our technique to DNA and proteins to measure, for the first time, the conductance of DNA and proteins trapped between two electrodes using DEP by in situ monitoring the impedance change of the DNA and protein solutions in both solution and dry states. This technique contains the rudimentaries of single molecule transistor fabrication with an essentially nanoelectrochemistry approach (Fan and Bard, 1995; Bard and Faulkner, 2001). What is new about this paper is:

(1) It is the first measurement of the conductivity of DNA after ac DEP manipulation.
(2) It is the highest frequency DEP experiment to date on DNA by an order of magnitude.
(3) It is the first ever measurement of the electrical properties of any protein.
(4) It is the first measurement of the crossover frequency from positive to negative DEP of 20 nm diameter nanoparticles (previously the crossover frequency was measured for 93 nm nanoparticles and aggregates of 14 nm beads).
(5) It is a new application of an old technique (DEP) to fabricate nanocircuits using ac voltages at the molecular scale.

In Fig. 1, we show a scale drawing of the three objects manipulated in this article: nanoparticles, DNA, and BSA protein. Although we are taking the first initial steps in this paper, it should be noted that these are mere "baby steps" towards electronic control of the assembly of matter into circuits at the molecular scale.

2. Materials and methods

2.1. Electrode design and fabrication

For our experiments, electrodes were fabricated using photolithography onto microscope cover slides. Ti (10 nm)/Au (100 nm) bilayers were deposited with electron-beam evaporation and lifted off in acetone. The geometry of the electrodes was designed for both positive and negative DEP experiments. For negative DEP, Huang and Pethig (Huang and Pethig, 1991) have shown that a planar, "quadrupole" electrode geometry allows the trapping of particles under the influence of negative DEP in the center of the electrodes, called the "trap". This is because there is an electric field gradient minimum in region of the center of the electrodes, and particles undergoing negative DEP are repelled from the higher field regions.

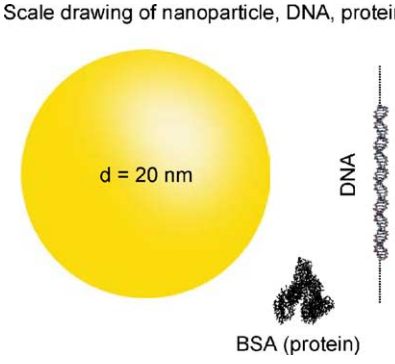

Fig. 1. Scale drawing of objects manipulated in this paper.

We have also performed numerical simulations for our electrode geometry, which is slightly different from the geometry considered by Huang. We find that the electric field gradient is maximum in the region closest to the electrode edges. Thus, for particles which undergo positive DEP, they should be attracted to those regions.

2.2. Sample preparation

Solutions containing either fluorescently labeled λ-phage DNA, BSA protein, or 20 nm latex beads were prepared as described below. An aliquot was placed on the cover slip with electrodes, which is then covered by a second slip. This configuration was necessary for the inverted microscope configuration used. An rf function generator (Stanford Research Systems, model DS 345) was used to apply electric fields in the frequency range of 10 kHz to 30 MHz, and applied voltages of up to 10 V.

2.3. Optical interrogation

The solution was imaged through an inverted Nikon TE200 microscope, equipped with a 40×/1.3 NA objective. Fluorescent images used epi-illumination with a mercury arc lamp providing the excitation. A back-illuminated, slow-scan, cooled CCD camera (AP7P, from Apogee Instruments) captured the images.

2.4. Electronic interrogation

After trapping, the low frequency (13 Hz) conductance between two electrodes was measured simultaneously while applying the ac electric field. The circuit used for the measurement is shown in Fig. 2. The high frequency electric field was used to trap the DNA or protein between the electrode gaps. A small amplitude, ac voltage was simultaneously applied and a lock-in-analyzer (Stanford Research Systems, model SR830) simultaneously measured the 13 Hz ac current. The 13 Hz current was monitored continuously as the solution dried in order to measure the conductance in both the wet and dry state.

In the experiments described in this paper, the measured conductance corresponds to a large number of molecules trapped electronically between the electrode gaps. While the fluorescence imaging experiments clearly

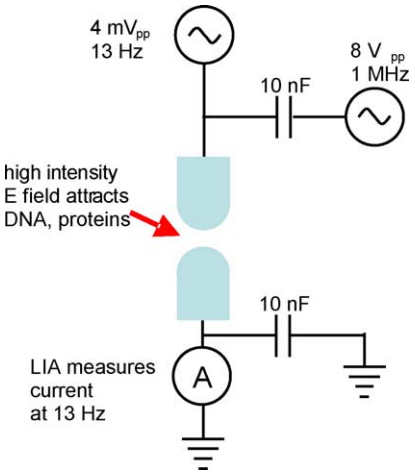

Fig. 2. Circuit for conductance measurements.

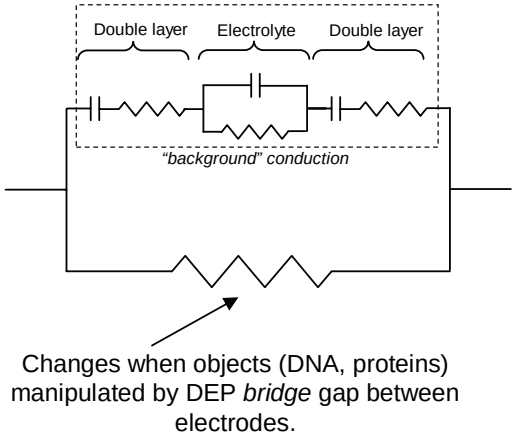

Fig. 4. Effective circuit model for objects trapped using DEP between electrodes.

and unambiguously demonstrate the presence of a large number of molecules of either DNA or proteins present in the gap between the electrodes, it remains for future work to provide more quantitative estimates for the number of molecules trapped and to push to the single molecule limit (Zheng et al., 2003). In Fig. 3, we show a schematic physical picture of the process of the DEP trapping.

The impedance between the electrodes consists of two parts, which we indicate in Fig. 4: first, there is the impedance of the electrolyte, which is a complicated function of frequency. In particular, at low frequencies, this impedance is dominated by the capacitance of the electrode–electrolyte interface. This impedance, which has been described in detail in Bard and Faulkner (2001), is not of prime interest in our work here. We are primarily interested in the fabrication of circuits, which can function even in the dry state, and at dc. The electrode–electrolyte impedance at dc forms a cell (battery) which we are not concerned with in this paper.

If the objects manipulated by DEP come into physical contact with both electrodes, then there will be a second, parallel conduction path, due to the impedance of the object *itself*. Generally, this impedance will dominantly be *resistive*, and hence relatively frequency independent. Because we are interested primarily in this resistive impedance, we chose a low probe frequency. However, we choose not to probe at dc, because the electrochemical effects (polarization of the electrode) at dc would mask the resistive impedance we are interested in. Thus, the frequency of 13 Hz was chosen to measure this second, resistive component.

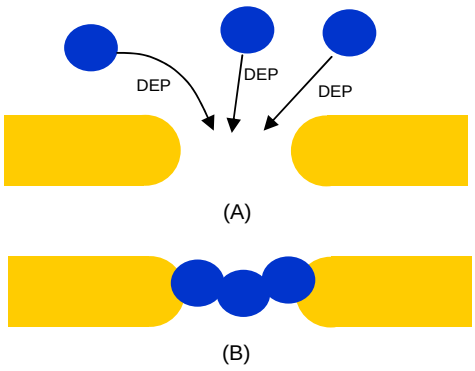

Fig. 3. Schematic of DEP trapping process. In this paper, the balls represent proteins and DNA.

3. Results: DNA

3.1. DNA: optical measurements

The DNA used in the experiments was λ-phage DNA (48.5 kbp). The DNA solution was prepared as follows: λ-phage DNA (Promega Corporation, Madison, WI) was purchased in a buffer solution of 10 mM Tris–HCl, 10 mM NaCl, 1 mM EDTA, at a concentration of 500 μg/ml. The solution was diluted 5×10^5 times with DI water. SYBR green was then added to the solution for the fluorescence measurements. The suspension conductivity was 1 mS/m.

We observed that DNA under our experimental conditions undergoes positive DEP (i.e. is attracted to high electric field intensity regions) for a range of frequencies between 100 kHz and 30 MHz. Below 100 kHz, no effect was observed. We did not observe DNA to undergo negative DEP under our experimental conditions. We show in Fig. 5 images of successive on/off/on/off conditions of DNA which has been trapped in the high-field region between electrodes with a 10 μm gap. We clearly observe positive DEP (i.e. the DNA is attracted to high electric field intensity regions) over a range of frequencies between 100 kHz and 1 MHz.

We have repeated this experiment dozens of times with electrodes with central gaps of 5, 10 and 20 μm. With four electrode geometries with 50 μm gaps, we were unable to see any effect of the electric fields on the DNA for applied voltages of up to 8 V. This is consistent with the scaling arguments presented above: large electrodes are less effective

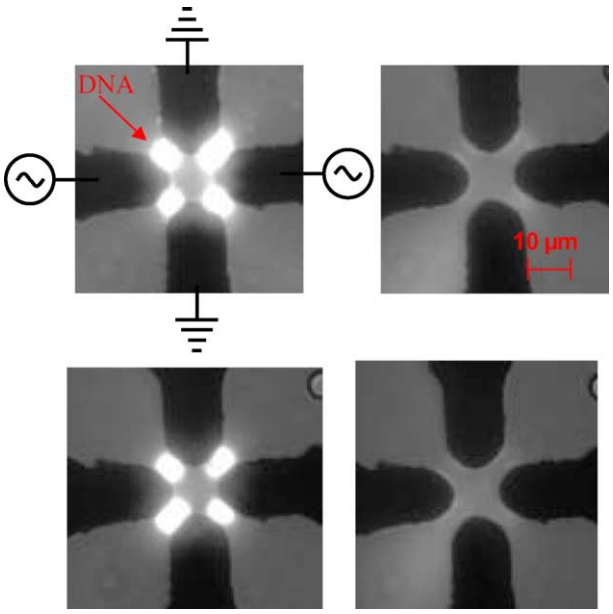

Fig. 5. Images of fluorescently labeled DNA. The four images were taken in on/off/on/off sequence in a time span of about 30 s ($f = 1$ MHz, applied voltage = 8 V).

in trapping nanosized objects than smaller electrodes. We have also been able to trap DNA using interdigitated, castellated electrodes with 10 μm gaps. DNA was only observed to undergo positive DEP with those electrodes, as well.

3.2. DNA: electronic measurements

λ-Phage DNA stretched is 17 μm long, but in its native state it is a randomly coiled ball about 2–4 μm in diameter. In our experiments the gap between the electrodes was less than 5 μm at the nearest point, so we expect that the DNA is stretched out and connects to both electrodes.

In a separate experiment, we applied an aliquot of solution to the electrodes and monitored the 13 Hz current as per the circuit diagram in Fig. 2. A "background" current of 227 nA was measured in the absence of the high frequency signal, due to the background conductivity of the electrolyte, indicated in the dotted lines in Fig. 4. This background signal is expected to be only weakly dependent on whether the DNA molecules bridge the gap between the electrodes on the surface of the sample. In fact, the reason we use DI water in the experiments presented in this paper is to minimize this background conductance.

Then, while monitoring the 13 Hz current in situ, a 1 MHz ac electric field was applied to trap DNA between the electrodes. Based on the optical interrogation measurements presented in the previous section, we are confident that the DNA is indeed collected between the electrodes. After trapping the DNA with the 1 MHz field, no change in the 13 Hz current was measured within a resolution of 0.1 nA. We monitored the current as the solution dried over a period of 72 h. After the solution dried the measured current was below the noise level of the measurement (0.1 nA). This corresponds to an upper limit of 25 nS for the conductance indicated by the large resistor in Fig. 4 for the DNA. This work represents the first such measurement of the conductance of DNA after trapping with an ac electric field.

In order to verify that the DNA is indeed trapped electronically, we have conducted a set of control experiments. An aliquot of DNA solution with a concentration of 10^{-6} μg/ml was dropped onto one sample with quadrupole electrodes. For a control sample, DI water was dropped onto a similar set of electrodes. An ac bias of 8 V at 1 MHz was applied to both samples. Both the DNA solution and DI water were dried in air while the voltage was still being applied. The samples were then imaged in an SEM; the SEM pictures are shown in Fig. 6. The dark material between the electrodes shown in Fig. 6A is not seen in the control electrodes shown in Fig. 6B. Since the DNA solution is composed of only λ-phage DNA and DI water, we believe that the dark material is DNA itself.

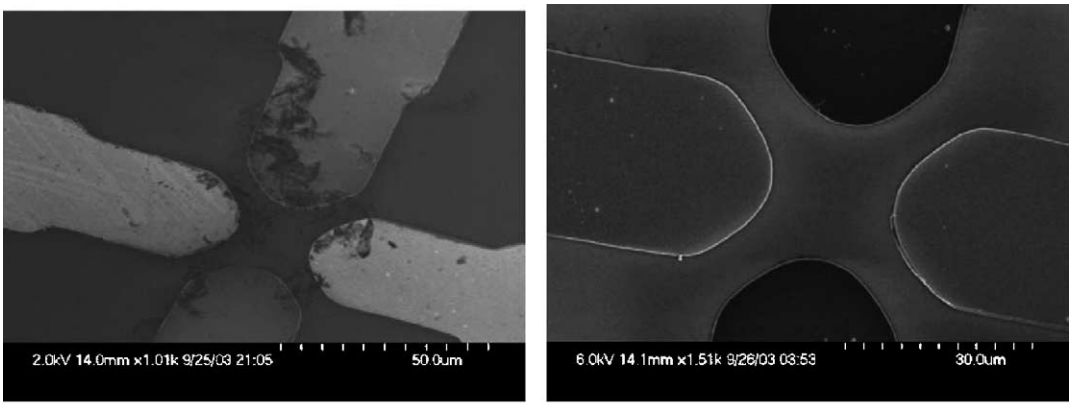

Fig. 6. (A) Sample SEM image after drying when DNA solution was used. (B) Sample SEM image after drying when only DI water was used.

4. Results: proteins

4.1. Proteins: optical measurements

For the protein experiments, the sample was prepared as follows: bovine serum albumin (BSA, molecular weight 68 kDa) labeled with tetramethylrhodamine (Molecular Probes, Eugene, OR) was dissolved in DI water at a concentration of 1 mg/ml and centrifuged. The supernatants were diluted to 1 μg/ml with DI water. The suspension conductivity was 1 mS/m.

We observed that BSA underwent positive DEP for frequencies between 50 kHz and 5 MHz. Negative DEP was not observed at lower frequencies under our experimental conditions. The frequency range of 200–300 kHz was observed to be most effective at attracting the BSA to the high-electric field regions. We show in Fig. 7 images of successive on/off/on/off conditions of BSA which has been trapped in the high-field region between electrodes with a 10 μm gap. We clearly observe positive DEP (i.e. the BSA is attracted to high electric field intensity regions) over a range of frequencies between 50 kHz and 5 MHz. We have repeated this experiment dozens of times with electrodes with central gaps of 5, 10 and 20 μm. With four electrode geometries with 50 μm gaps, we were unable to see any effect of the electric fields on the BSA for applied voltages of up to 8 V.

4.2. Proteins: electronic measurements

In its folded state BSA should be roughly spherical in geometry with diameter of order 10 nm. Previous work of Washizu has shown that high intensity electric fields can change the conformational state of certain proteins (Washizu et al., 1992), however the effect of the high-intensity electric field on BSA is unknown. While we were unable to image single BSA molecules under our current experimental setup, it is clear that a large number of BSA molecules were attracted to the gap between the electrodes. With this in mind we measured the conductance at 13 Hz to determine whether it was possible to electrically interrogate the BSA.

In a separate experiment, we applied an aliquot of protein solution to the electrodes and monitored the 13 Hz current as per the circuit diagram in Fig. 2. A "background" current of 2.5 nA was measured in the absence of the high frequency signal, due to the background conductivity of the electrolyte, indicated in the dotted lines in Fig. 4. (This background current was less than the background current in the case of the DNA because we used smaller aliquot of solution.) This background signal is expected to be only weakly dependent on whether the protein molecules bridge the gap between the electrodes on the surface of the sample.

Then, while monitoring the 13 Hz current in situ, a 1 MHz ac electric field was applied to trap protein between the electrodes. Based on the optical interrogation measurements presented in the previous section, we are confident that the protein is indeed collected between the electrodes. After trapping the protein with the 1 MHz field, no change in the 13 Hz current was measured within a resolution of 1 pA. We monitored the current as the solution dried over a period of 24 h. After the solution dried the measured current was below the noise level of the measurement (0.1 nA). This corresponds to an upper limit of 25 nS for the conductance indicated by the large resistor in Fig. 4. This work represents the first such measurement of the conductance of any protein after trapping with an ac electric field.

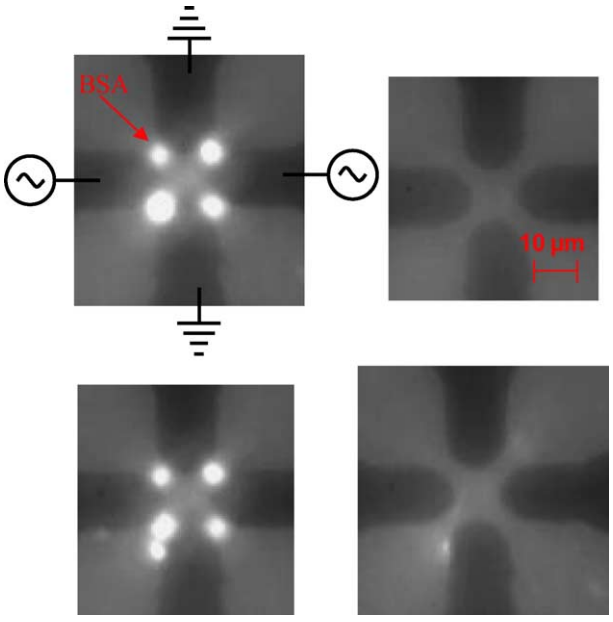

Fig. 7. Images of BSA protein in a span of about 30 s (f = 200 kHz, applied voltage = 8 V).

5. Results: nanoparticles

In a final set of experiments we were able to use DEP to manipulate fluorescently labeled latex beads of diameter 20 nm (Molecular Probes, Eugene, OR) suspended in DI water. The suspension conductivity was 1 mS/m. Latex beads have served as an ideal test-bed for the use of DEP at the micron and submicron scale (Muller et al., 1996; Green and Morgan, 1997a,b) and serve as convincing evidence that under our experimental conditions it is indeed possible to manipulate submicron objects.

For the 20 nm beads, we found that the beads undergo positive DEP for frequencies between 500 kHz and 22 MHz, while above 22 MHz the beads undergo negative DEP. We show in Fig. 8 an image of beads undergoing negative DEP, with an applied frequency of 22 MHz. The beads are seen to be trapped in the center of the electrodes. In Fig. 9, we show an image of beads under the influence of positive DEP, where they are clearly seen attracted to the region of high electric field intensity between the electrodes.

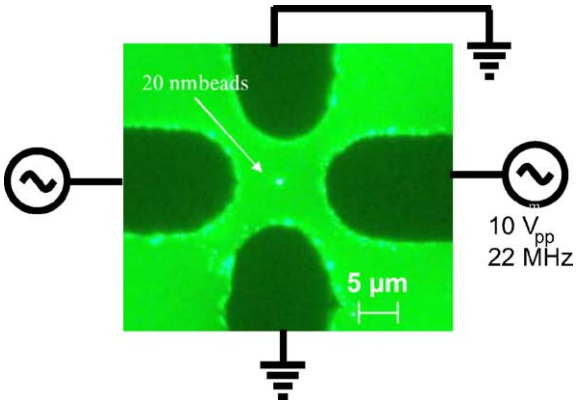

Fig. 8. Twenty nanometer latex beads shown trapped in the center of the electrodes due to negative DEP.

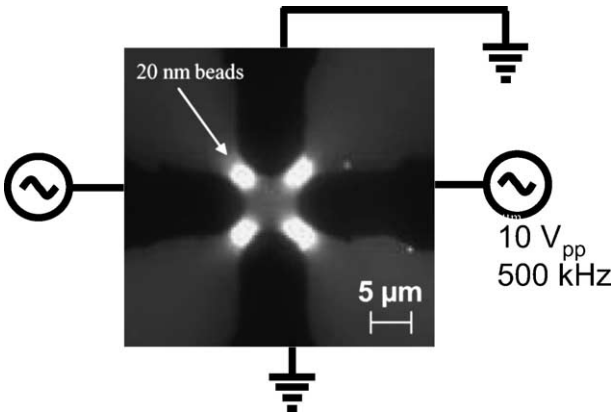

Fig. 9. Twenty nanometer latex beads shown attracted to high electric field regions between the electrodes.

6. Summary of results: DEP spectrum

In Fig. 10 below, we show the resulting spectrum for positive versus negative DEP for the three objects measured. This is the DEP "spectrum".

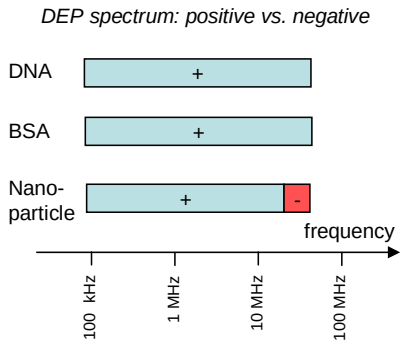

Fig. 10. DEP spectrum, showing frequency regions where positive (+) and negative (−) DEP were observed. Thirty megahertz was the upper frequency limit for our electronics.

7. Discussion: nanoparticles

We begin our discussion of the nanoparticle results, as they are the simplest to interpret. A key initial question is whether the nanoparticles form aggregates. Previous research using DEP on 14 nm latex beads found that the particles form aggregates (Muller et al., 1996), while work on single 93 nm beads was reported in (Green and Morgan, 1997b). Because of the spatial resolution limits of optical microscopy it is very difficult to determine if aggregates are formed using optical microscopy alone. However, we have independent evidence that, under our experimental conditions, the 20 nm beads do not form aggregates. In a separate experiment (Zheng et al., 2004a), we used nanotube electrodes to trap 20 nm beads and then imaged them with a scanning electron microscope. Under the SEM, we see no evidence whatsoever for aggregation. Thus, we believe the 20 nm beads are not aggregated.

The frequency dependence of the nanoparticle experiments is given in Fig. 10; in sum we find positive DEP at frequencies below 22 MHz and negative DEP at frequencies above 22 MHz. In order to interpret this result, we use Eqs. (1)–(5) as the basis for our analysis. Our experimental result for the crossover frequency corresponds theoretically to the frequency at which the Clausius–Mossotti factor crosses from positive to negative.

The frequency dependence of the Clausius–Mossotti factor (Eq. (2)) is determined by the frequency dependence of the complex medium and particle dielectric constants. The real part of the medium dielectric constant can be taken as 78.5 and independent of frequency over the range of interest. Similarly, the real part of the dielectric constant of the nanoparticles can be taken as 2.55, and independent of frequency over the range of interest. The frequency dependence of the CM factor is thus determined entirely by the imaginary part of the dielectric constants, which we discuss next.

For the medium, the conductivity is known, so the imaginary part of the medium dielectric constant is known. For the nanoparticle, the bulk conductivity is negligible. However, the surface of the nanoparticle has a negative static charge density, which attracts counter-ions from the solution. These can be bound to the surface of the nanoparticle (the Stern layer) or occur as a diffuse cloud. Eq. (5) provides a means of estimating the effect of both these counter-ion concentrations, provided an effective surface conductivity (K_s) is known for these counter-ions. In general predicting the numerical value of K_s is difficult. Green and Morgan measured its value on larger nanoparticles (93–557 nm) and found it to be of order 1 nS (Green and Morgan, 1999). If we assume this value is appropriate also for the 20 nm nanoparticles in our experiments, we can predict the frequency-dependent CM factor for our experiments. This prediction is shown in Fig. 11 below. The predicted crossover frequency (which can also be calculated analytically from Eq. (4)) of 30 MHz is close to our experimentally measured crossover frequency of 22 MHz. Given the fact that the surface conductivity K_s

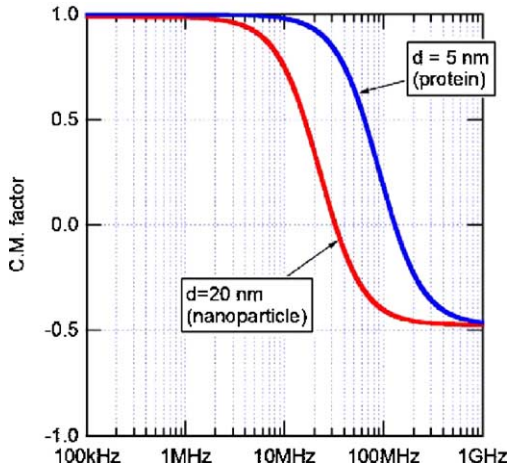

Fig. 11. Frequency dependence of the Clausius–Mossotti factor, assuming a surface conductance of $K_s = 1$ nS.

is not known independently, this is a reasonable agreement with previous experiments and theoretical predictions.

While we do not know whether the surface conductance is due predominantly to the bound or diffuse counter-ions, the agreement between the theoretical and experimental crossover frequency seems to indicate that bound counter-ions contribute the dominant portion. The diffuse cloud of counter-ions extends a Debye length between the particle and medium. The Debye length is given by

$$\lambda_{\text{Debye}} = \sqrt{\frac{\varepsilon k_B T}{2e^2 n}}. \quad (7)$$

For our solutions, this corresponds to 100 nm, much larger than the particle diameter. In our prediction for the crossover frequency, we have neglected the finite thickness of the diffuse cloud of counter-ions, and we still find reasonable agreement with experiment. The bound counter-ions will not significantly change the effective diameter of the nanoparticle for the DEP crossover frequency used in Eq. (5). This leads us to conclude that bound counter-ions dominate the surface conduction K_s.

Our experiments were performed in a medium with low conductivity, 1 mS/m. Based on Eq. (4), we can predict the dependence of the crossover frequency on the medium conductivity. This prediction, together with our experimentally measured crossover frequency, is shown in Fig. 12 below. Armed with this understanding of the frequency dependence of DEP of the 20 nm beads and the effect of the charge double layer, we move on next to analyze the experiments on the proteins.

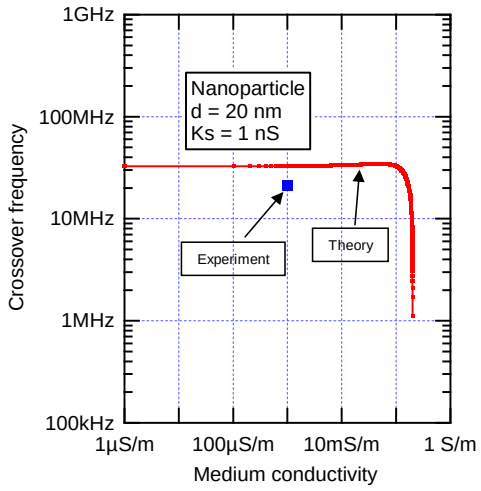

Fig. 12. Predicted dependence of DEP crossover frequency on suspension conductivity.

8. Discussion: proteins

Our analysis of the protein DEP measurements proceeds along the lines of the 20 nm nanoparticle measurements. For simplicity we model the albumin protein as a sphere of diameter 5 nm; this should be expected to yield semi-quantitative results. Using this model allows us to apply the analysis based on Eqs. (1)–(6) for spherical particles. For our protein experiments, the charge double layer and surface conductivity play a critical role. As with the latex bead experiments, the surface conductivity of the bound or diffuse counter-ions is difficult to predict from first principles. If we use our results from the 20 nm latex beads as guide, we can estimate a reasonable value for the surface conductivity of 1 nS. Based on this estimate, and assuming the bulk conductivity of the protein is negligible, we calculate a spectrum for the CM factor shown as the blue curve in Fig. 11. (This curve is insensitive to the numerical value of the real part of the dielectric constant for the protein.) This curve, and also Eq. (4), predicts a crossover frequency of ≈100 MHz, which is larger than the frequency range used in these experiments. This is entirely consistent with our experimental results: we observe

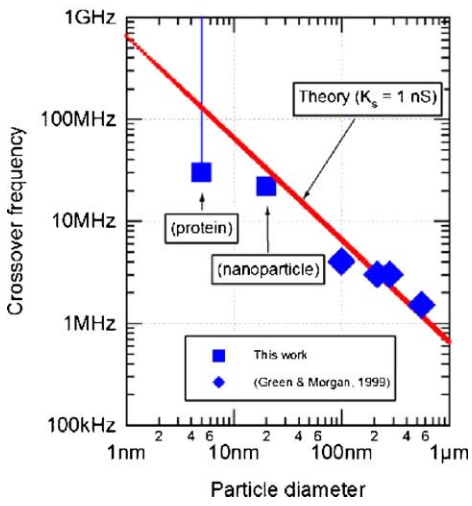

Fig. 13. Crossover frequency vs. particle diameter in the low suspension conductivity limit. The measurement for the protein crossover frequency corresponds to a lower limit only, limited by the electronics used, thus the bar.

only positive DEP for the proteins measured up to 30 MHz, i.e. we observe a positive CM factor.

We are now in a position to integrate our nanoparticle experiments, those of Green and Morgan, and our protein experiments into a unified understanding of the role of the double layer and particularly the surface conductance in determining the crossover frequency for the application of DEP to nanoparticles. In Fig. 13 we plot our measured crossover frequency (in the low suspension-conductivity limit) as a function of particle diameter, as well as that measured by Green (Green and Morgan, 1999) for larger diameter nanoparticles. Remarkably, the data are all consistent with Eq. (4), assuming a surface conductance of 1 nS.

9. Discussion: DNA

Unlike proteins, DNA cannot be reasonably modeled as a spherical particle. Under the influence of DEP it is known the DNA is stretched into a long, thin configuration, i.e. it is not randomly coiled. In this section, we provide some elementary discussions of the DEP on DNA, using a simple model for the surface conductivity as we did for the proteins. The failure of this simple model to explain our experimental results indicates that a fundamental understanding of the mechanism of DEP in manipulating DNA is still lacking.

The polarization factor used in Eq. (1), and hence the Clausius–Mossotti factor given in Eq. (2), are only applicable to spherical particles. In this section we model DNA as an ellipsoid which allows us to use analytical results for the polarization. Based on the induced dipole for an ellipsoid, which can be calculated analytically (Stratton, 1941), we define an "effective" Clausius–Mossotti factor, given by (Jones, 1995)

$$K_{\text{effective}}(\omega) \equiv Re\left[\frac{\varepsilon_{\text{p}}^* - \varepsilon_{\text{m}}^*}{3[A(\varepsilon_{\text{p}}^* - \varepsilon_{\text{m}}^*) + \varepsilon_{\text{m}}^*]}\right], \tag{8}$$

where A is the depolarization factor. For an ellipsoid with cylindrical symmetry, it can be shown that A is given by

$$A = \frac{1-e^2}{2e^3}\left[\log\left(\frac{1+e}{1-e}\right) - 2e\right], \tag{9}$$

where

$$e \equiv \sqrt{1-\left(\frac{b}{a}\right)^2}, \tag{10}$$

and a and b are the major and minor axis of the ellipsoid.

A question which arises in this context, which has not been addressed to our knowledge, is what effect the charge double layer and the surface conductivity plays in the case of DEP of an ellipsoidal object. O'Konski has provided general arguments (Okonski, 1960) that the induced dipole moment can be calculated using the effective CM factor given in Eq. (8), provide the particle conductivity is given by an analog of Eq. (5):

$$\sigma_{\text{p}} = \sigma_{\text{b}} - \frac{2K_{\text{s}}}{b}. \tag{11}$$

Here b is the minor axis of the ellipsoid.

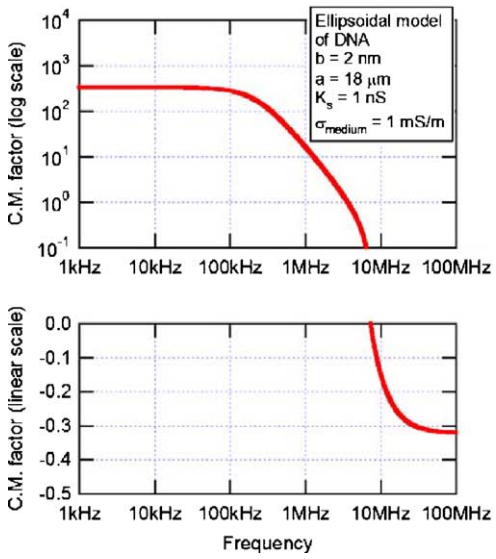

Fig. 14. Calculated effective CM factor for DNA, assuming an ellipsoidal model with $a = 2$ nm, $b = 18$ μm, and $K_{\text{s}} = 1$ nS.

We now discuss the implications of O'Konski's model in the case of DEP: first, and most importantly, the effective CM factor given by Eq. (8) is no longer bound between +1 and −0.5 as is the case with a spherical particle. This is consistent with the well-known polarizability of long, oblate objects. Second, the crossover from positive to negative DEP is a non-trivial function of the particle geometry and surface conductivity. In order to illustrate this, we have calculated the effective CM factor for a reasonable model of stretched DNA. We assume $b = 2$ nm, $a = 18$ μm, and $K_{\text{s}} = 1$ nS. We also assume a medium conductivity of 1 mS/m. Based on this model, we plot in Fig. 14 the CM factor versus frequency. A crossover frequency from positive to negative DEP is predicted at 6 MHz, and a large polarizability is predicted at low frequencies. In our prediction we did not take into account the Debye length, which is of order 100 nm for low conductivity solutions. If we assume the double layer has a finite thickness of order 100 nm (by taking $b = 100$ nm), with surface conductivity still of order 1 nS, the crossover frequency is still of order 1 MHz. The crossover frequency is only weakly dependent on the medium conductivity and surface conductivity. To our knowledge, the CM factor for an ellipsoid which takes into account O'Konski's prediction for the surface conductivity of the double layer has not been previously considered.

The large, low frequency polarizability is consistent with much of the work on DEP manipulation of DNA to date, as discussed in the introductory section. However, the crossover frequency is in disagreement with our experiments, as well

as almost all published experiments on DNA. In our experiments show that DNA undergoes positive DEP up to 30 MHz, whereas all previous experiments on DEP of DNA were done below 2 MHz. In this sense our experiments extend the range of data for DEP of DNA by over an order of magnitude in frequency.

In our experiments, the gap between electrodes is less than the stretched length of DNA. Thus, the mathematical treatment of DNA as a simple point–dipole should not be expected to give quantitatively meaningful results; the method of moments in this case should be replaced by a different, perhaps numerical technique. However, this does not explain the discrepancy with other experiments, for example Washizu's, where the distance between electrodes was much larger than the length of the stretched DNA. We are thus led to conclude that a simple model of DNA as an ellipsoid with an electrical double layer at the surface described by a surface conductivity simply fails to explain many experimental results, ours included. A fundamental understanding of the molecular basis of DEP manipulation of DNA is still lacking.

10. Conclusions

In this work we have described the electronic manipulation of proteins, DNA, and nanoparticles, and applied these for the first time to measure an upper limit on the conductance of DNA and protein molecules that were manipulated with DEP to bridge a gap between electrodes. Our measurements find that DNA and protein is very insulating. Based on former work by Green and Morgan, we have applied a unified description of the double layer and its effect on the crossover frequency of nanoparticles and proteins, remarkably consistent with previous experiments on DEP manipulation of somewhat larger nanoparticles. Finally, we have pointed out the lack of a fundamental understanding of the DEP manipulation of DNA, and argued that the current model of a simple surface conductivity due to a charge double layer is not consistent with experiment. Looking generally towards the future, our technique for electronically controlled circuit assembly presented herein may be useful for shorter DNA strands or other molecular scale devices, especially when integrated with nanowire and nanotube electrodes (Zheng et al., 2003, 2004a,b).

Acknowledgements

This work was supported by the US National Science Foundation, the ARO, the ONR, and DARPA. We thank Alan Lee for assistance with the experiments.

References

Alivisatos, A.P., Johnsson, K.P., Peng, X.G., Wilson, T.E., Loweth, C.J., Bruchez, M.P., Schultz, P.G., 1996. Organization of 'nanocrystal molecules' using DNA. Nature 382, 609–611.

Allsopp, D.W.E., Milner, K.R., Brown, A.P., Betts, W.B., 1999. Impedance technique for measuring dielectrophoretic collection of microbiological particles. J. Phys. D: Appl. Phys. 32, 1066–1074.

Amlani, I., Rawlett, A.M., Nagahara, L.A., Tsui, R.K., 2002. An approach to transport measurements of electronic molecules. Appl. Phys. Lett. 80, 2761–2763.

Asbury, C.L., Diercks, A.H., van den Engh, G., 2002. Trapping of DNA by dielectrophoresis. Electrophoresis 23, 2658–2666.

Asbury, C.L., van den Engh, G., 1998. Trapping of DNA in nonuniform oscillating electric fields. Biophys. J. 74, 1024–1030.

Bard, A.J., Faulkner, L.R., 2001. Electrochemical Methods: Fundamentals and Applications. Wiley, New York.

Bezryadin, A., Dekker, C., 1997. Nanofabrication of electrodes with sub-5 nm spacing for transport experiments on single molecules and metal clusters. J. Vacuum Sci. Technol. B 15, 793–799.

Bezryadin, A., Dekker, C., Schmid, G., 1997. Electrostatic trapping of single conducting nanoparticles between nanoelectrodes. Appl. Phys. Lett. 71, 1273–1275.

Bezryadin, A., Westervelt, R.M., Tinkham, M., 1999. Self-assembled chains of graphitized carbon nanoparticles. Appl. Phys. Lett. 74, 2699–2701.

Bhatt, K.H., Velev, O.D., 2004. Control and modeling of the dielectrophoretic assembly of on-chip nanoparticle wires. Langmuir 20, 467–476.

Braun, E., Eichen, Y., Sivan, U., Ben-Yoseph, G., 1998. DNA-templated assembly and electrode attachment of a conducting silver wire. Nature 391, 775–778.

Brown, A.P., Milner, K.R., Allsopp, D.W.E., Betts, W.B., 1998. Characteristic dielectrophoretic collection of 20 nm latex beads measured by an impedance technique. Electron. Lett. 34, 1934–1936.

Bubke, K., Gnewuch, H., Hempstead, M., Hammer, J., Green, M.L.H., 1997. Optical anisotropy of dispersed carbon nanotubes induced by an electric field. Appl. Phys. Lett. 71, 1906–1908.

Burke, P.J., 2004. Nano-dielectrophoresis: Electronic Nanotweezers In: Nalwa, H.S. (Ed.), Encyclopedia of Nanoscience and Nanotechnology. American Scientific, Stevenson Ranch, CA.

Cai, L.T., Tabata, H., Kawai, T., 2000. Self-assembled DNA networks and their electrical conductivity. Appl. Phys. Lett. 77, 3105–3106.

Chen, J., Reed, M.A., 2002. Electronic transport of molecular systems. Chem. Phys. 281, 127–145.

Chen, X.Q., Saito, T., Yamada, H., Matsushige, K., 2001. Aligning single-wall carbon nanotubes with an alternating-current electric field. Appl. Phys. Lett. 78, 3714–3716.

Chou, C.F., Tegenfeldt, J.O., Bakajin, O., Chan, S.S., Cox, E.C., Darnton, N., Duke, T., Austin, R.H., 2002. Electrodeless dielectrophoresis of single- and double-stranded DNA. Biophys. J. 83, 2170–2179.

Debye, P., Debye, P.P., Eckstein, B.H., 1954a. Dielectric high-frequency method for molecular weight determinations. Phys. Rev. 94, 1412–1412.

Debye, P., Debye, P.P., Eckstein, B.H., Barber, W.A., Arquette, G.J., 1954b. Experiments on polymer solution in inhomogeneous electrical fields. J. Chem. Phys. 22, 152–153.

de Pablo, P.J., Moreno-Herrero, F., Colchero, J., Herrero, J.G., Herrero, P., Baro, A.M., Ordejon, P., Soler, J.M., Artacho, E., 2000. Absence of dc-conductivity in lambda-DNA. Phys. Rev. Lett. 85, 4992–4995.

Dewarrat, F., Calame, M., Schonenberger, C., 2002. Orientation and positioning of DNA molecules with an electric field technique. Single Mol. 3, 189–193.

Diehl, M.R., Yaliraki, S.N., Beckman, R.A., Barahona, M., Heath, J.R., 2001. Selfassembled, deterministic carbon nanotube wiring networks. Angew. Chem. Int. Ed. 41, 353.

Duan, X.F., Huang, Y., Cui, Y., Wang, J.F., Lieber, C.M., 2001. Indium phosphide nanowires as building blocks for nanoscale electronic and optoelectronic devices. Nature 409, 66–69.

Eisenstadt, M., Scheinberg, I.H., 1972. Dielectrophoresis of macromolecules—determination of diffusion constant of poly-gamma-benzyl-l-glutamate. Science 176, 1335.

Eisenstadt, M., Scheinberg, I.H., 1973. Dielectrophoresis of macromolecules. Biopolymers 12, 2491–2512.

Fan, F.R.F., Bard, A.J., 1995. Electrochemical detection of single molecules. Science 267, 871–874.

Fink, H.W., Schonenberger, C., 1999. Electrical conduction through DNA molecules. Nature 398, 407–410.

Germishuizen, W.A., Walti, C., Tosch, P., Wirtz, R., Pepper, M., Davies, A.G., Middelberg, A.P.J., 2003a. Dielectrophoretic manipulation of surface-bound DNA. IEE Proc. Nanobiotechnol. 150, 54–58.

Germishuizen, W.A., Walti, C., Wirtz, R., Johnston, M.B., Pepper, M., Davies, A.G., Middelberg, A.P.J., 2003b. Selective dielectrophoretic manipulation of surface-immobilized DNA molecules. Nanotechnology 14, 896–902.

Green, N.G., Morgan, H., 1997a. Dielectrophoretic investigations of sub-micrometre latex spheres. J. Phys. D: Appl. Phys. 30, 2626–2633.

Green, N.G., Morgan, H., 1997b. Dielectrophoretic separation of nano-particles. J. Phys. D: Appl. Phys. 30, L41–L44.

Green, N.G., Morgan, H., 1998. Separation of submicrometre particles using a combination of dielectrophoretic and electrohydrodynamic forces. J. Phys. D: Appl. Phys. 31, L25–L30.

Green, N.G., Morgan, H., 1999. Dielectrophoresis of submicrometer latex spheres. 1. Experimental results. J. Phys. Chem. B 103, 41–50.

Green, N.G., Ramos, A., Morgan, H., 2000. AC electrokinetics: a survey of submicrometre particle dynamics. J. Phys. D: Appl. Phys. 33, 632–641.

Heath, J.R., Ratner, M.A., 2003. Molecular electronics. Phys. Today 56, 43–49.

Hermanson, K.D., Lumsdon, S.O., Williams, J.P., Kaler, E.W., Velev, O.D., 2001. Dielectrophoretic assembly of electrically functional microwires from nanoparticle suspensions. Science 294, 1082–1086.

Holzel, R., Bier, F.F., 2003. Dielectrophoretic manipulation of DNA. IEE Proc. Nanobiotechnol. 150, 47–53.

Holzel, R., Gajovic-Eichelmann, N., Bier, F.F., 2003. Oriented and vectorial immobilization of linear M13 dsDNA between interdigitated electrodes—towards single molecule DNA nanostructures. Biosens. Bioelectron. 18, 555–564.

Huang, Y., Pethig, R., 1991. Electrode design for negative dielectrophoresis. Meas. Sci. Technol. 2, 1142–1146.

Hughes, M.P., 2000. AC electrokinetics: applications for nanotechnology. Nanotechnology 11, 124–132.

Hughes, M.P., 2002. Dielectrophoretic behavior of latex nanospheres: low-frequency dispersion. J. Colloid Interface Sci. 250, 291–294.

Hughes, M.P., Flynn, M.F., Morgan, H., 1999a. Dielectrophoretic measurements of submicrometre latex particles following surface modification. Electrostatics 163, 81–84.

Hughes, M.P., Green, N.G., 2002. The influence of Stern layer conductance on the dielectrophoretic behavior of latex nanospheres. J. Colloid Interface Sci. 250, 266–268.

Hughes, M.P., Morgan, H., 1999. Dielectrophoretic characterization and separation of antibody coated submicrometer latex spheres. Anal. Chem. 71, 3441–3445.

Hughes, M.P., Morgan, H., Flynn, M.F., 1999b. The dielectrophoretic behavior of submicron latex spheres: influence of surface conductance. J. Colloid Interface Sci. 220, 454–457.

Jones, T.B., 1995. Electromechanics of Particles. Cambridge University Press, Cambridge.

Kabata, H., Kurosawa, O., Arai, I., Washizu, M., Margarson, S.A., Glass, R.E., Shimamoto, N., 1993. Visualization of single molecules of RNA-polymerase sliding along DNA. Science 262, 1561–1563.

Kabata, H., Okada, W., Washizu, M., 2000. Single-molecule dynamics of the *Eco*RI enzyme using stretched DNA: its application to in situ sliding assay and optical DNA mapping. Jpn. J. Appl. Phys. Part 1: Regul. Pap. Short Notes Rev. Pap. 39, 7164–7171.

Kasumov, A.Y., Kociak, M., Gueron, S., Reulet, B., Volkov, V.T., Klinov, D.V., Bouchiat, H., 2001. Proximity-induced superconductivity in DNA. Science 291, 280–282.

Lee, S.W., Bashir, R., 2003. Dielectrophoresis and electrohydrodynamics-mediated fluidic assembly of silicon resistors. Appl. Phys. Lett. 83, 3833–3835.

Losche, A., Hultschig, H., 1955. Dielekrophorese in Flussigkeiten. Kolloid-Zeitschrift 141, 177–187.

Luo, Y., Collier, C.P., Jeppesen, J.O., Nielsen, K.A., Delonno, E., Ho, G., Perkins, J., Tseng, H.R., Yamamoto, T., Stoddart, J.F., Heath, J.R., 2002. Two-dimensional molecular electronics circuits. Chemphyschem 3, 519.

Lyklema, J., 2000. Fundamentals of Interface and Colloid Science. Academic Press, San Diego.

Lyklema, J., Dukhin, S.S., Shilov, V.N., 1983. The relaxation of the double-layer around colloidal particles and the low-frequency dielectric-dispersion. 1. Theoretical considerations. J. Electroanal. Chem. 143, 1–21.

Lyklema, J., Springer, M.M., Shilov, V.N., Dukhin, S.S., 1986. The relaxation of the double-layer around colloidal particles and the low-frequency dielectric-dispersion. 3. Application of theory to experiments. J. Electroanal. Chem. 198, 19–26.

Milner, K.R., Brown, A.P., Allsopp, D.W.E., Betts, W.B., 1998. Dielectrophoretic classification of bacteria using differential impedance measurements. Electron. Lett. 34, 66–68.

Mirkin, C.A., Letsinger, R.L., Mucic, R.C., Storhoff, J.J., 1996. A DNA-based method for rationally assembling nanoparticles into macroscopic materials. Nature 382, 607–609.

Morgan, H., Green, N.G., 2003. Electrokinetic Technologies for Sub-Micron Particles. Research Studies Press, Philadelphia, PA.

Muller, T., Gerardino, A., Schnelle, T., Shirley, S.G., Bordoni, F., DeGasperis, G., Leoni, R., Fuhr, G., 1996. Trapping of micrometre and sub-micrometre particles by high frequency electric fields and hydrodynamic forces. J. Phys. D: Appl. Phys. 29, 340–349.

Nagahara, L.A., Amlani, I., Lewenstein, J., Tsui, R.K., 2002. Directed placement of suspended carbon nanotubes for nanometer-scale assembly. Appl. Phys. Lett. 80, 3826–3828.

Namasivayam, V., Larson, R.G., Burke, D.T., Burns, M.A., 2002. Electrostretching DNA molecules using polymer-enhanced media within microfabricated devices. Anal. Chem. 74, 3378–3385.

Okahata, Y., Kobayashi, T., Tanaka, K., Shimomura, M., 1998. Anisotropic electric conductivity in an aligned DNA cast film. J. Am. Chem. Soc. 120, 6165–6166.

Okonski, C.T., 1960. Electric properties of macromolecules. 5. Theory of ionic polarization in polyelectrolytes. J. Phys. Chem. 64, 605–619.

Pethig, R., 1996. Dielectrophoresis: using inhomogeneous AC electrical fields to separate and manipulate cells. Crit. Rev. Biotechnol. 16, 331–348.

Pethig, R., Markx, G.H., 1997. Applications of dielectrophoresis in biotechnology. Trends Biotechnol. 15, 426–432.

Pohl, H.A., 1978. Dielectrophoresis: The Behavior of Neutral Matter in Nonuniform Electric Fields. Cambridge University Press, Cambridge.

Porath, D., Bezryadin, A., de Vries, S., Dekker, C., 2000. Direct measurement of electrical transport through DNA molecules. Nature 403, 635–638.

Prock, A., Mcconkey, G., 1960. Inhomogeneous field method for the study of large polarizable particles. J. Chem. Phys. 32, 224–236.

Ramos, A., Morgan, H., Green, N.G., Castellanos, A., 1998. AC electrokinetics: a review of forces in microelectrode structures. J. Phys. D: Appl. Phys. 31, 2338–2353.

Schwarz, G., 1962. A theory of low-frequency dielectric dispersion of colloidal particles in electrolyte solution. J. Phys. Chem. 66, 2636.

Shimamoto, N., 1999. One-dimensional diffusion of proteins along DNA—its biological and chemical significance revealed by single-molecule measurements. J. Biol. Chem. 274, 15293–15296.

Smith, P.A., Nordquist, C.D., Jackson, T.N., Mayer, T.S., Martin, B.R., Mbindyo, J., Mallouk, T.E., 2000. Electric-field assisted assembly and alignment of metallic nanowires. Appl. Phys. Lett. 77, 1399–1401.

Storm, A.J., van Noort, J., de Vries, S., Dekker, C., 2001. Insulating behavior for DNA molecules between nanoelectrodes at the 100 nm length scale. Appl. Phys. Lett. 79, 3881–3883.

Stratton, J.A., 1941. Electromagnetic Theory. McGraw-Hill Book Company Inc., New York.

Suehiro, J., Yatsunami, R., Hamada, R., Hara, M., 1999. Quantitative estimation of biological cell concentration suspended in aqueous medium by using dielectrophoretic impedance measurement method. J. Phys. D: Appl. Phys. 32, 2814–2820.

Suzuki, S., Yamanashi, T., Tazawa, S., Kurosawa, O., Washizu, M., 1998. Quantitative analysis of DNA orientation in stationary AC electric fields using fluorescence anisotropy. IEEE Trans. Ind. Appl. 34, 75–83.

Tour, J.M., 2000. Molecular wires for electronics applications: a review. Polym. News 25, 329–336.

Tsukahara, S., Yamanaka, K., Watarai, H., 2001. Dielectrophoretic behavior of single DNA in planar and capillary quadrupole microelectrodes. Chem. Lett. 250–251.

Ueda, M., Iwasaki, H., Kurosawa, O., Washizu, M., 1999a. Atomic force microscopy observation of deoxyribonucleic acid stretched and anchored onto aluminum electrodes. Jpn. J. Appl. Phys. Part 1: Regul. Pap. Short Notes Rev. Pap. 38, 2118–2119.

Ueda, M., Yoshikawa, K., Doi, M., 1997. Stretching of long DNA under alternating current electric fields in a concentrated polymer solution. Polym. J. 29, 1040–1043.

Ueda, M., Yoshikawa, K., Doi, M., 1999b. Molecular motion of long deoxyribonucleic acid chains in a concentrated polymer solution depending on the frequency of alternating electric field. Polym. J. 31, 637–644.

Wakaya, F., Nagai, T., Gamo, K., 2002. Position control of carbon nanotube using patterned electrode and electric field. Microelectron. Eng. 63, 27–31.

Washizu, M., Kurosawa, O., 1990. Electrostatic manipulation of DNA in microfabricated structures. IEEE Trans. Ind. Appl. 26, 1165–1172.

Washizu, M., Kurosawa, O., Arai, I., Suzuki, S., Shimamoto, N., 1995. Applications of electrostatic stretch-and-positioning of DNA. IEEE Trans. Ind. Appl. 31, 447–456.

Washizu, M., Shikida, M., Aizawa, S., Hotani, H., 1992. Orientation and transformation of flagella in electrostatic-field. IEEE Trans. Ind. Appl. 28, 1194–1202.

Winfree, E., Liu, F.R., Wenzler, L.A., Seeman, N.C., 1998. Design and self-assembly of two-dimensional DNA crystals. Nature 394, 539–544.

Yamamoto, K., Akita, S., Nakayama, Y., 1996. Orientation of carbon nanotubes using electrophoresis. Jpn. J. Appl. Phys. Part 2: Lett. 35, L917–L918.

Yamamoto, K., Akita, S., Nakayama, Y., 1998. Orientation and purification of carbon nanotubes using ac electrophoresis. J. Phys. D: Appl. Phys. 31, L34–L36.

Yamamoto, T., Kurosawa, O., Kabata, H., Shimamoto, N., Washizu, M., 2000. Molecular surgery of DNA based on electrostatic micromanipulation. IEEE Trans. Ind. Appl. 36, 1010–1017.

Zheng, L., Li, S., Brody, J.P., Burke, P.J., 2004a. Manipulating nanoparticles in solution with electrically contacted nanotubes using dielectrophoresis. unpublished.

Zheng, L., Li, S., Burke, P.J., 2004b. Self-assembled gold nanowires from nanoparticles. unpublished.

Zheng, L., Li, S., Burke, P.J., Brody, J.P., 2003. Towards single molecule manipulation with dielectrophoresis using nanoelectrodes. In: Proceedings of the Third IEEE Conference on Nanotechnology, vol. 1, pp. 437–440.

Zimmermann, U., Neil, G.A., 1996. Electromanipulation of Cells. CRC Press, Boca Raton, FL.